

# 1 Introduction

This experiment explores the use of transducers, a device that can convert mechanical energy into electrical energy. Transducers are useful for observing quantities that are otherwise impossible to measure by taking an input of mechanical energy (in this case, resulting strain of a cantilever beam from a bending moment) and converting it to an output voltage. For this experiment, a design was created to utilize strain gages in order to determine an input tension in a tensiometer. To ensure the design would be effective, theoretical calculations were done beforehand surrounding the dimensions of the tensiometer. The design of the tensiometer is detailed more in the sections below (Figure 2). It is essentially a cable connected on either end to a Instron Loading Machine, and then weaved through three pins built into the tensiometer. Four strain gages are then wired from the tensiometer into a P3 Strain Indicator. The connection used is known as a full bridge strain gage circuit, which is detailed in section 4.3.3 of the Model P3 Strain Indicator and Recorder Instruction Manual [2]. This circuit allows the strain to be measured by the P3 Indicator after an applied load is placed on the tensiometer by the Instron Loading Machine stretching the cable. After results were obtained from the actual experiment, they were compared to the theoretical numbers calculated beforehand and placed into a graph. Overall, the purpose of the experiment was to be familiarized with the use of transducers and strain gages by designing a tensiometer that output a tension based on strain.

## 2 Theory

In this project, an applied load was measured through utilization of strain gauges. Strain gauges have been used since the mid 1800s to determine resulting forces by way of changing resistances in a circuit. In a Wheatstone bridge, the relationship between a change in resistance and strain is defined as

$$\frac{\Delta R}{R_0} = k\varepsilon \quad (1)$$

where  $\Delta R$  is the difference in resistance before and after the applied load,  $R_0$  is the initial resistance,  $k$  is the gage factor which is a characteristic of the strain gage, and  $\varepsilon$  is the desired strain. The ratio of the output and input voltage is defined as

$$\frac{U_A}{U_E} = \frac{R_1 R_3 - R_2 R_4}{(R_1 + R_2)(R_3 + R_4)} \quad (2)$$

where  $U_A$  is the bridge output voltage and  $U_E$  is the bridge input voltage. Before any applied load, assuming all resistances are the same, there will be no output. As more displacement occurs due to an applied load, there will be a change in element resistances and therefore there will also be an output voltage associated with that change. This change in voltage directly correlates with a change in resistance as seen in Ohm's law, which is

$$V = IR \quad (3)$$

where  $V$  is the voltage drop across a resistor element,  $I$  is the current across the element, and  $R$  is the resistance of the element. Substituting (1) into (2) the resulting equation is

$$\frac{U_A}{U_E} = \frac{k}{4}(\varepsilon_1 - \varepsilon_2 + \varepsilon_3 - \varepsilon_4) \quad (4)$$

where  $\varepsilon_1, \varepsilon_2, \varepsilon_3, \varepsilon_4$  represent element strains. Figure (1) below shows respective resistor elements where  $R_1, R_2, R_3, R_4$  correspond to  $\varepsilon_1, \varepsilon_2, \varepsilon_3, \varepsilon_4$  respectively.

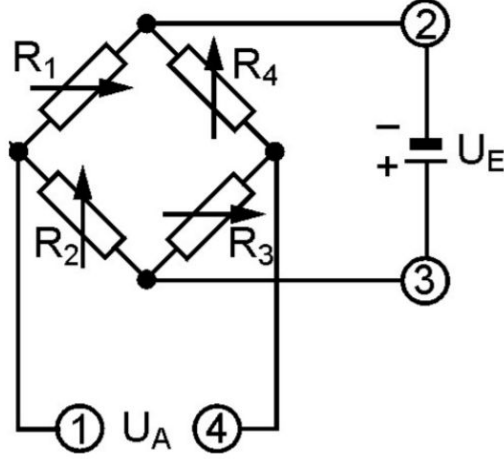


Figure 1: Wheatstone Bridge Circuit

The design of the tensiometer was determined through cantilever beam calculations. An excel file was created to assist in this process. A total of nine input parameters were used in the excel file including  $L, D, t, r, G, T, E, \sigma_y$ , and  $x$ . These inputs were then utilized in the output cells to determine the design parameters. First, the effective length of the cantilever,  $l_c$ , was determined through the following relation

$$l_c = 0.375L - 0.375 \quad (5)$$

where  $L$  is the outer pin center to center distance and  $0.375L$  was determined by a design choice that the cantilever beam length would be about 75% of half the distance between the outer pin centers. An extra 0.375 inches is subtracted since the center of the middle pin will be placed 0.375 inches away from the end of the cantilever to provide support for the pin to thread into. This choice was made so that there would be substantial material to support the base of the cantilever; thus effectively isolating the location of deflection primarily to the cantilever. Second, the height of the cantilever,  $h$ , was found by multiplying plate thickness by the ratio of  $\frac{h}{t}$  where  $t$  is the thickness of the plate. Plate thickness was determined by choosing a thickness greater than the width of two strain gages since this project requires two strain gages on either side of the cantilever beam. Third, the area moment of inertia,  $I_a$ , for a cantilever beam was calculated as

$$I_a = \frac{th^3}{12} \quad (6)$$

The fourth step involved calculating the deflection angle  $\theta$ . Figure (2) below shows  $\theta$  as the angle between the cable and a line tangent with the outer diameter of all of the shoulder bolts.

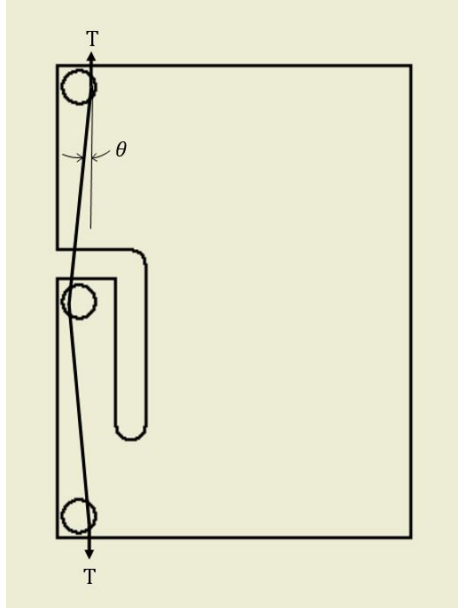


Figure 2: Tensiometer Reference Diagram

Figure (3) below corresponds to the following two equations used to find  $\theta$  and  $F$

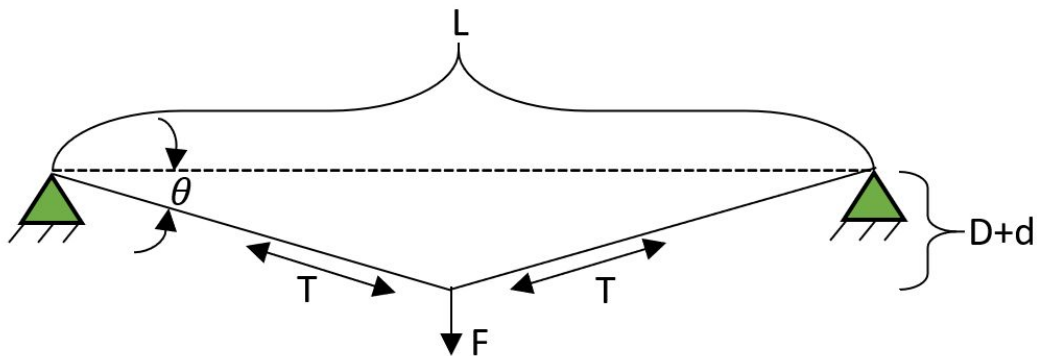


Figure 3: Geometrical Cable Tension Model

where  $T$  represents the cable tension,  $F$  is the pin load on the cantilever pin,  $D$  is pin diameter,  $d$  is cable diameter, and  $\theta$  is the fixed cable deflection angle. The dimensions of this rigging tensiometer was designed around a theoretical cable tension of 2,000 lbs. Since the cable has an apparent diameter, a more detailed geometric analysis is necessary to calculate  $\theta$ . Figure (4) below shows a close-up diagram of the cable passing over two pins.

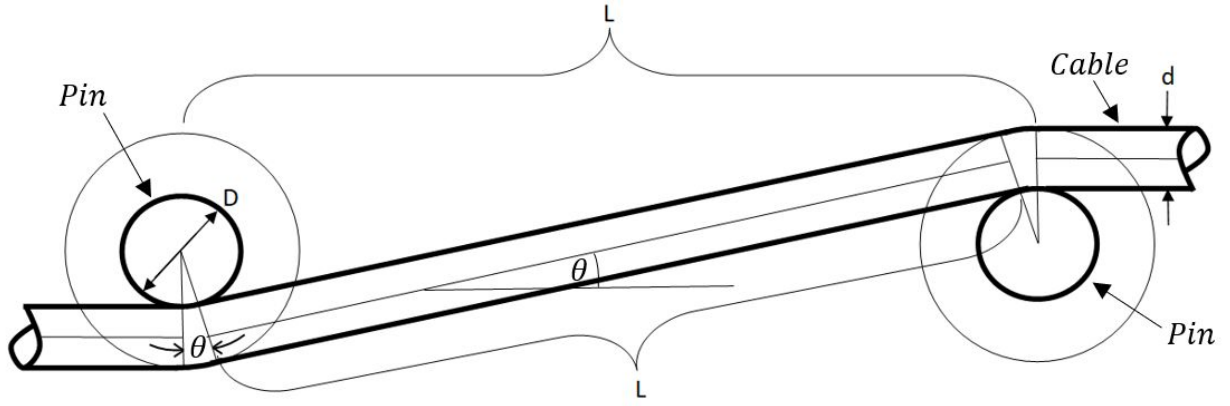


Figure 4: Detailed Cable Tension Model

$\theta$  is then calculated from geometry assuming no deflection at the cantilever beam. The equation

$$\theta = \sin^{-1}\left(\frac{D+d}{L/2}\right) \quad (7)$$

was used to find  $\theta$ . Fifth, the pin load on the cantilever due to cable tension,  $F$ , was calculated by the following relation:

$$F = 2T \sin(\theta) \quad (8)$$

Cantilever stress,  $\sigma$ , at the strain gauges was determined in the sixth step by the following relation

$$\sigma = \frac{Mc}{I} = \frac{6M}{th^2} \quad (9)$$

where  $M = F(l_c - x)$ . Seventh, microstrain,  $\mu\epsilon$ , was calculated by the following relation

$$\mu\epsilon = \frac{1000000\sigma}{E} \quad (10)$$

where  $E$  is the modulus of elasticity of 6061 aluminum. Eighth, cantilever beam deflection,  $y$ , was calculated by the following relation

$$y = \frac{Fl_c^3}{12EI} \quad (11)$$

Ninth, safety factor,  $S$ , was calculated by the simple relation

$$S = \frac{\sigma_y}{\sigma} \quad (12)$$

To quantify the error in the angle of the actual deflection, the corrected cable angle,  $\theta'$  was found by the following relation.

$$\theta' = \tan^{-1}\left(\frac{2(D-y)}{L}\right) \quad (13)$$

The % difference of assumed cable deflection angle and corrected cable deflection angle was found by the following relation.

$$\% \text{ Difference} = \frac{\theta - \theta'}{\theta'} \quad (14)$$

By substituting equations (11) and (9) into (4), the relationship between the input and output voltage as a function of the input force at the pin can be described as

$$\frac{U_A}{U_E} = \frac{6kF(l_c - x)}{Eth^2} \quad (15)$$

Therefore, the resulting force at the pin as a function of the ratio of the output and input voltages can be mathematically expressed as

$$F = \frac{U_A}{U_E} \cdot \frac{Eth^2}{6k(l_c - x)} \quad (16)$$

Finally, we can substitute equation (4) and (8) into (16) to relate strain at the location of the strain gage centroid to the cable tension in the following equation

$$|\epsilon| = \frac{6(2T \sin(\theta))(l_c - x)}{Eth^2} \quad (17)$$

## 2a Design and Construction

The equations derived above were inserted into a spreadsheet as functions and were used to determine the dimensions of the tensiometer. The design was theoretically calculated to withstand a cable tension of 2,000 *lbs<sub>f</sub>* with a safety factor of 2.99. Figure (5) below shows the spreadsheet that was used in the design of the tensiometer:

	A	B	C	D	E	F	G
1	<b>Input Parameter</b>						
2	L (in)	7.25	Outer pin center to center distance				
3	D (in)	0.375	Pin diameter				
4	d (in)	0.09375	Cable Diameter				
5	t (in)	0.5	Plate thickness				
6	r	2	Ratio of h/t				
7	G (in)	0.492126	Effective strain Gage Length				
8	T (lb)	2000	Trial tension value				
9	E (psi)	1.00E+07	Modulus of elasticity				
10	σ <sub>y</sub> (ksi)	36	Yield strength				
11	x (in)	0.4063	Location of strain gage centroid				
12							
13	<b>Output Values</b>						
14	l <sub>c</sub> (in)	2.344	Length of cantilever				
15	h (in)	1	Cantilever x-sect height				
16	I (in <sup>4</sup> )	0.04166666667	Moment of inertia				
17	Θ (rad)	0.1296734537	Fixed cable deflection angle (assumes no cantilever deflection)				
18	F (lb)	517.2413793	Pin load on cantilever, due to cable tension (assuming no cantilever deflection)				
19	σ (ksi)	12.02555172	Cantilever stress at strain gages				
20	ε (με)	1,202.56	Micro strain = 1 million times stress/modulus				
21	y (in)	0.001332	Cantilever deflection				
22							
23	Θ' (rad)	0.1293060453	Corrected cable deflection angle by adding deflection				
24	% Error	0.28%	% difference of assumed cable deflection angle and corrected cable deflection				
25							
26	S	2.993625642	Safety Factor				

Figure 5: Design Spreadsheet

Technical drawing of a 3A3 Tensiometer. The drawing includes a front view (top left), a side view (top right), a detail of the mounting bracket (bottom left), and a detail of the sensor assembly (bottom right). Dimensions are given in inches.

**Front View (Top Left):** Shows a rectangular body with a central slot. Dimensions: 1.00 (width of slot), 6.00 (length of slot), .50 (thickness of body).

**Side View (Top Right):** Shows the thickness of the body and the mounting bracket. Dimensions: .313 (thickness of body), 3.63 (height of mounting bracket), 8.00 (total height), 5/16-18 THRU TAP (thread specification), .56 (diameter of mounting hole), .50 (width of mounting bracket).

**Detail of Mounting Bracket (Bottom Left):** Shows a bracket with a central slot and a mounting hole. Dimensions: .50 (width of slot), 2.72 (height of slot), .375 (width of mounting hole), R.25 (radius of corner).

**Detail of Sensor Assembly (Bottom Right):** Shows a sensor with a central slot and a mounting hole. Dimensions: .313 (thickness of body), 3.63 (height of mounting bracket), 8.00 (total height), 5/16-18 THRU TAP (thread specification), .56 (diameter of mounting hole), .50 (width of mounting bracket).

**Table:**

UNLESS OTHERWISE SPECIFIED:		NAME	DATE
DIMENSIONS ARE IN INCHES		DRAWN	
TOLERANCES:		CHECKED	
FRACTIONAL: ±		ENG APPR.	
ANGULAR: MACH ±		ENG APPR.	
DECIMAL: ±		QA	
THREE PLACE DECIMAL: ±		COMMENTS:	
INTERPRET GEOMETRIC TOLERANCING PER:			
MATERIAL:			
FINISH:			
NEXT ASSY	USED ON		
APPLICATION			
DO NOT SCALE DRAWING			

**PROPRIETARY AND CONFIDENTIAL**  
THE INFORMATION CONTAINED IN THIS DRAWING IS THE SOLE PROPERTY OF < NGRI COMPANY NAME HERE >. ANY REPRODUCTION IN PART OR AS A WHOLE WITHOUT THE WRITTEN PERMISSION OF < NGRI COMPANY NAME HERE > IS PROHIBITED.

**3A3 Tensiometer**

SIZE DWG. NO. REV  
SCALE: 1:4 WEIGHT: SHEET 1 OF 1

Once the design was complete, a 6061-T6 aluminum block and three alloy steel shoulder screws were purchased through McMaster-Carr and construction began. A JET milling machine was used to mill the cantilever beam and handle as shown below in Figure (7):



Figure 7: JET Milling Machine

A close up view of the aluminum block is shown below in Figure (8) partway through the milling process:



Figure 8: Aluminum Block Close Up View

Next, the shoulder screw holes were drilled using a drill press and then tapped using a 5/16"-18 drill tap. Figure (9) below shows the drill press was used to help center the tap as it went through the first few threads:





Figure 9: Tap Centering

When tapping holes, it is sometimes difficult to maintain perpendicularity when tapping the first few threads. That is why the center of the top of the drill tap was aligned with the help of the drill press. Cutting fluid was used for all manufacturing processes to reduce wear on tools and provide cleaner cuts.

Strain gages were then attached by first degreasing the desired surface of application with CSM-1. Second, conditioner A: M-Prep and 320 grit sandpaper was used to wet-sand the surface. The residue was wiped with gauze. Conditioner A: M-Prep was used again with 400 grit sandpaper. The location of the strain gages was scribed with pencil lead and then the surface was wiped with conditioner A and a cotton swab. Neutralizer 5A was applied on the surface and wiped with gauze. Cellophane tape was applied to the top of the strain gages to hold them and then they were placed onto the desired location, with copper tabs facing up. The tape was then partially removed at a shallow angle, such that the entire strain gage was pivoted about its short edge but still connected to the specimen at its edge by the tape. A thin film of blue catalyst-B 200 was applied to the bottom of the strain gage and then a dab of M-Bond was placed at the base of the strain gage. With a paper towel, the strain gage was immediately placed onto the desired location and pressure was applied for one minute then it was allowed to cure for an additional two minutes before removing the tape at a sharp angle to ensure the strain gage stays on the specimen. 5-6 ft of wire was cut for the strain gages (each strain gage needs two wires). Each wire end was stripped, twisted and tinned with solder (flux was used for all solder joints) . The gage terminals were tinned and the wires were soldered to the gage terminals. Finally the other ends of the wires were configured for a full-bridge wheatstone arrangement as shown in Figure (1).



## 2b Sensitivity, Range and Excitation Voltage

Sensitivity,  $S$ , was calculated by the following equation which was found on page 53 of [1]:

$$S = \frac{d}{V_i} \quad (18)$$

Where  $d$  is the smallest increment that can be measured and used confidently to accurately predict the tension in the cable and  $V_i$  is the excitation voltage. Twenty-five data points were collected during the experiment where the readings from the P3 indicator showed increments of  $3 \mu\epsilon$  on average for each tension increment of 20 Newtons. A linear fit was determined in the presentation of results section; therefore, it can then be determined that if the tension increments were 6.67 Newtons instead of 20 Newtons, the P3 would read  $1 \mu\epsilon$ . Thus, the smallest increment chosen for the tensiometer project is  $d = 1 \mu\epsilon$ . According to [2], nominal bridge excitation voltage is 1.5 Volts DC.

Sensitivity can be calculated as

$$S = \frac{1 \times 10^3 \mu\epsilon}{1.5V} = 6.67 \times 10^{-4} V^{-1}$$

Range, which is the highest voltage that can be measured is found through the equation from page 54 of [1]:

$$V^* = \frac{d^*}{S} \quad (19)$$

Where  $V^*$  is the range and  $d^*$  is the maximum strain reading on the P3 indicator. The range is calculated as shown below:

$$V^* = \frac{31,000 \mu\epsilon}{6.67 \times 10^{-4} V^{-1}} = 4.65 \times 10^7 V \quad (20)$$

## 3 Experimental Apparatus and Procedures

The testing apparatuses used in this experiment are a P3 Strain Indicator and an Instron Model 5582. The P3 Strain Indicator utilizes a full Wheatstone Circuit to measure the resulting strain on an object due to an external force with a maximum capacity of  $31,000 \mu\epsilon$ . [2] In order to use the P3 Strain Indicator to measure the strain resulting from the tensiometer, the strain gauges' leadwires must be correctly connected to the input terminals. The black arm on each respective terminal must be lifted. Then, the leadwire is inserted all the way into the terminal, and the arm is carefully lowered to clamp the wire to the terminal. Figure (10) below shows the front panel of the P3 strain indicator.

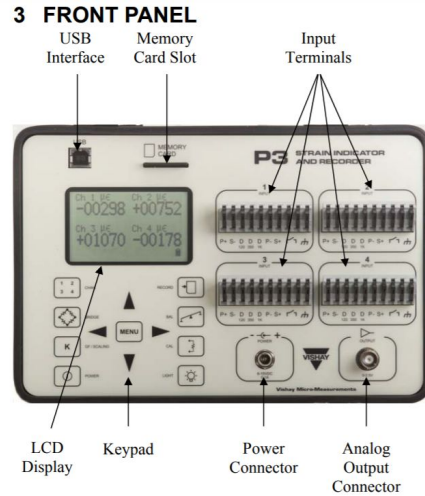


Figure 10: Front Panel of P3

Once all required connections have been made, the user must go into the settings of the P3 and change the system to use the full bridge configuration. The next step is to test the apparatus by using the Instron Model 5582. This apparatus is a large testing machine with a load capacity of 22,500  $lbf$ . [4] The 5582 column of Figure (11) shows loading and speed parameters in various units.

Parameter	Specifications			
	5581	5582	5584	5585H
Testing types	Tension, Compression and through zero operation. Standard configuration is below the moving crosshead. Not suitable for fatigue testing, but limited cyclic testing is available. Refer to "Cyclic Testing" on page 2-11. High frequency waveforms are subject to mechanical limitations of the load frame and may cause excessive wear on the load frame.			
Basic control mode	Closed loop position control.			
Load capacity kN kgf lbf	50 5100 11240	100 10000 22500	150 15000 33750	250 <sup>a</sup> 25000 56200
Maximum speed mm/min in/min	1000 40	500 20	750 30	500 20
Minimum speed mm/min in/min	0.001 0.00004	0.001 0.00004	0.001 0.00004	0.001 0.00004
Maximum force at Full speed kN kgf lbf	35 3570 7870	75 7650 16860	110 <sup>*</sup> 11215 24730	100 10200 22480
<sup>*</sup> 5584 - If operating at 100 V $\pm$ 10% service, these values may need to be reduced to 50% of load capacity due to electrical current limits.				
Maximum speed at Full load mm/min in/min	500 20	250 10	375 15	200 8

Figure 11: Instron Series 5580 System Performance [4].

The Instron testing apparatus is shown in Figure (12).

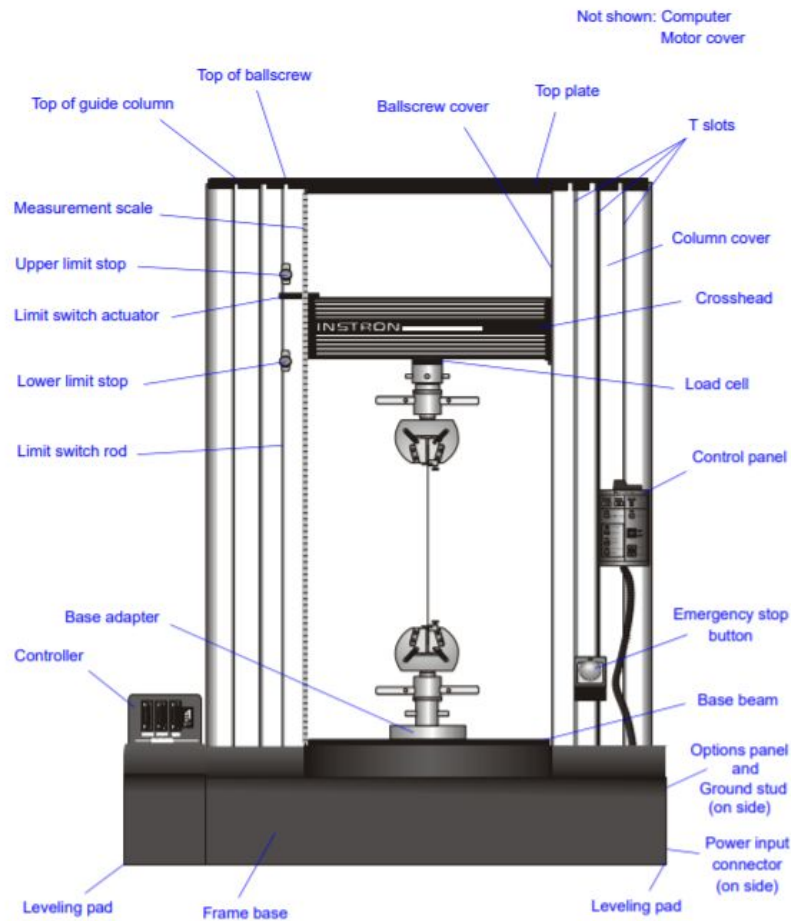
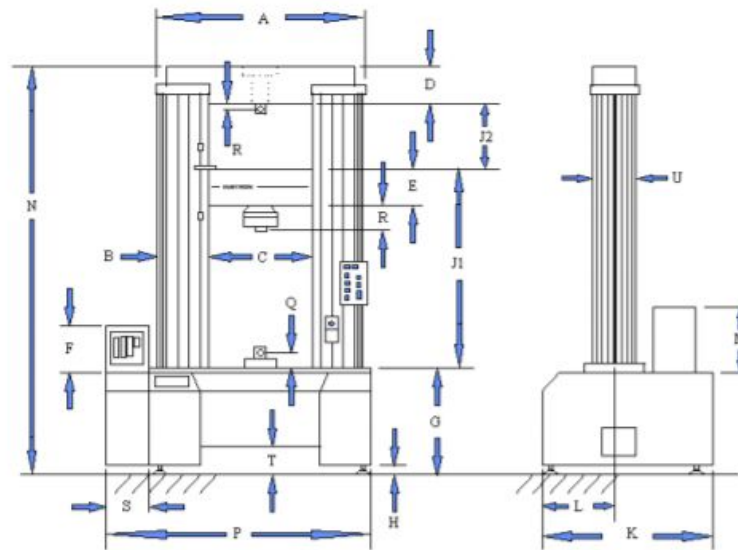


Figure 12: a) General Instron Series 5580 Load Frame Schematic [4](Top)  
b) Compression Plates and Control Panel (Bottom).

Figure (12a) shows a labeled general schematic of the Instron 5580 series with the tensile jaw attachment. Compression plates (see Figure (12b)) were used in this experiment to compress the vibrational isolators. The load cells indicated in Figure (12a) are high precision transducers that convert force into an electrical voltage. These load cells are attached to the crosshead and will collect force data and relay it to the controller as a compressive force is applied to the springs. Figure (13) shows the dimensions of the Instron Model 5582. Please see the Figure (13) Addendum in the appendix for the continued list of dimensions.



Designation	Description	Dimension mm (inch)
	Total crosshead travel 5581/5582 5584/5585H	1235 (48.6) 1182 (46.5)
	Vertical test daylight * 5581/5582 5584/5585H  * Measured from the base beam to the underside of the crosshead.	1310 (51.6) 1260 (49.6)
A	Across columns	1120 (44.1)
B	Column width	263 (10.4)
C	Horizontal test daylight	575 (22.6)
D	Top plate thickness	55 (2.2)

Figure 13: Instron Model 5582 Dimensions [4]

In order to complete the experiment, the Instron is first turned on with a switch located at the bottom right side of the base. After zeroing the Instron, input began from 0N and

increased by increments of 20N (4.5  $lbs_f$ ) until 500N. The force and strain at 25 data points were recorded.

## 4 Presentation of Results

Figure (14) below shows the theoretical vs. observed strain from the P3 indicator. Strain was recorded from the P3 at 25 data points from 0 to 500 Newtons in increments of 20 Newtons. The figure below shows tension values in lbs. The theoretical data was obtained using equation (17) in a spreadsheet for each tension load increment.

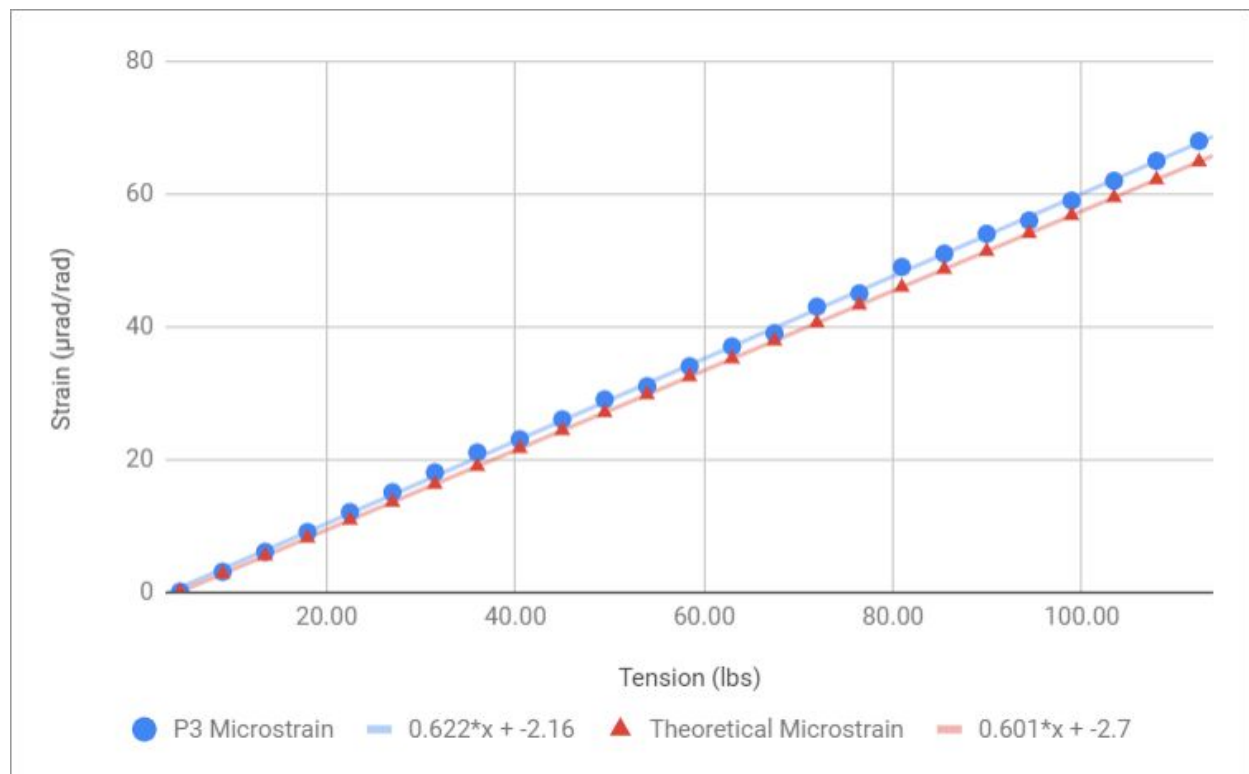


Figure 14: Theoretical vs. Observed Strain

Figure (15) below shows a finite element analysis simulation of the tensiometer under 10  $lbs_f$  of cable tension. Strain is represented as a color gradient and is quantified by the scale to the right of the tensiometer. This FEA simulation was conducted as an additional check to ensure the theory correctly predicts observed strain. The theory only predicts bending in the 2D plane but in reality there is a small torsional contribution from the load being placed out of the plane.

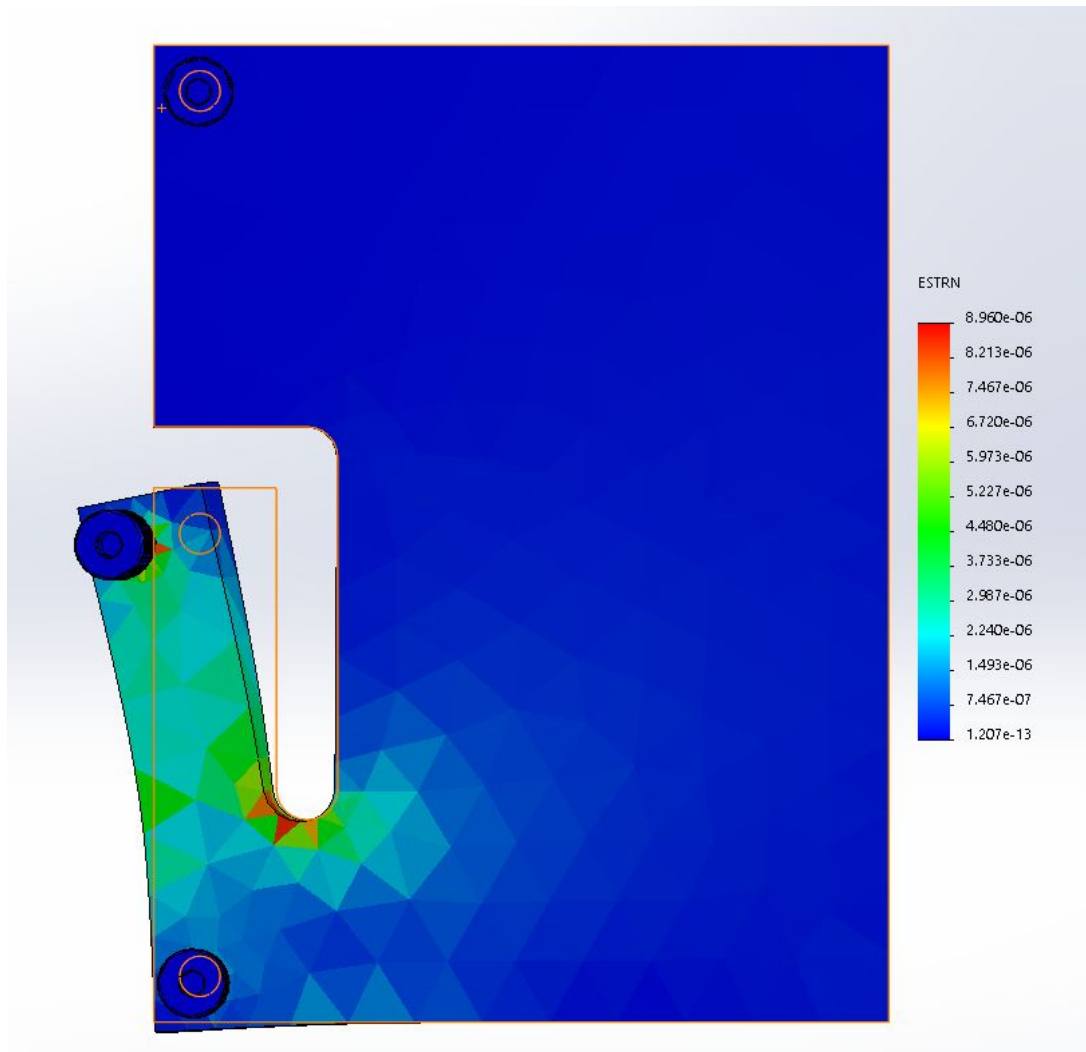


Figure 15: Finite Element Analysis of 10lbf Tension

Figure (16) below shows the predicted strain at the location of the strain gage centroids for a load of  $10 \text{ lbs}_f$  with the use of the spreadsheet mentioned earlier. The strain value for  $10 \text{ lbs}_f$  was calculated to compare the accuracy of the theoretical prediction to the strain shown in the FEA simulation.

	A	B	C	D	E	F	G
1	<b>Input Parameter</b>						
2	L (in)	7.25	Outer pin center to center distance				
3	D (in)	0.375	Pin diameter				
4	d (in)	0.09375	Cable Diameter				
5	t (in)	0.5	Plate thickness				
6	r	2	Ratio of h/t				
7	G (in)	0.492126	Effective strain Gage Length				
8	T (lb)	10	Trial tension value				
9	E (psi)	1.00E+07	Modulus of elasticity				
10	$\sigma_y$ (ksi)	36	Yield strength				
11	x (in)	0.4063	Location of strain gage centroid				
12							
13	<b>Output Values</b>						
14	l <sub>c</sub> (in)	2.344	Length of cantilever				
15	h (in)	1	Cantilever x-sect height				
16	I (in <sup>4</sup> )	0.04166666667	Moment of inertia				
17	$\Theta$ (rad)	0.1296734537	Fixed cable deflection angle (assumes no cantilever deflection)				
18	F (lb)	2.586206897	Pin load on cantilever, due to cable tension (assuming no cantilever deflection)				
19	$\sigma$ (ksi)	0.06012775862	Cantilever stress at strain gages				
20	$\epsilon$ ( $\mu\epsilon$ )	6.01	Micro strain = 1 million times stress/modulus				
21	y (in)	0.000007	Cantilever deflection				
22							
23	$\Theta'$ (rad)	0.1296716166	Corrected cable deflection angle by adding deflection				
24	% Error	0.00%	% difference of assumed cable deflection angle and corrected cable deflection				
25							
26	S	598.7251284	Safety Factor				

Figure 16: Predicted Strain at 10lbf for FEA Comparison

Table 1 below shows the sensitivity, range and excitation voltage calculated for the tensiometer/P3 assembly as discussed in section 2b, Sensitivity, Range, and Excitation Voltage.

Table 1: Sensitivity, Range and Excitation Voltage		
Sensitivity	Range	Excitation Voltage
$6.67 \times 10^{-4} \text{ V}^{-1}$	$4.65 \times 10^7 \text{ V}$	1.5 V

## 5 Uncertainty Analysis

Based on the data for theoretical and actual strain observed, the calculated values were quite accurate. The error in slopes of theoretical and actual strain was only observed to be 3.4%, an incredibly low value taking into consideration there were a few possible external sources of error. One example of a possible source of error has to do with the zeroing of the Instron. Since it was impossible to know when there was no tension in the rope used, the zeroing of the Instron was relative. As close to 0 as the true value of tension likely was, this would cause a systematic error of the force applied. Additionally, the theoretical equations used a simplified 2D model of the Tensiometer rather than a 3D one. If the force acted purely on the axis perpendicular to the strain, this would cause no problems. However, since the force is actually slightly vertical to this axis (due to the thickness of the rope and the placement of the screws), the resulting input would also



cause a moment in the perpendicular plane leading to torsional strain, albeit small relative to the input force. Finally, the friction of the cable was not accounted for in the theoretical calculations. The net force was assumed to be purely perpendicular, but friction would cause a force parallel to the observed axis. This force would cause the cable to bind, possibly outputting higher strain.

In terms of error related to material choice and properties, the used Modulus of Elasticity was merely an estimate and could vary with temperature or quality of material used. Additionally, the calculated values assumed a perfectly squared fillet of the tensiometer. The reality was that the edges were rounded, which would amplify the stiffness characteristics of the cantilever beam, resulting in less strain. Finally, the Modulus of Elasticity of the cable was not accounted for, which would affect how the cable reacted to input tension and the resulting output strain.

In comparing the Finite Element Analysis in Figure (15) with the calculated strain in Figure (16), the results are strikingly similar. The location of the centroid of the strain gages was determined to be .4063" from the base of the beam. The corresponding location in the FEA model shows a strain of about  $6.347 \mu\epsilon$ . The calculated value was 6.01, or an error of about 5.3%. The FEA model took into account the aforementioned out of plane strain that was induced by the vertical aspect of the tension force, thereby showing this additional force is negligible.

## **6 Discussion of Results**

In Figure (14) above, theoretical and observed values for strain as a function of input tension are compared. Both models show a linear fit with slightly different slopes. Overall, both the class of function of both models and the low error of 3.4% indicate that the theoretical model predicted the actual model quite well. Additionally, the FEA shown in Figure (15) lines up well with the calculation shown in Figure (16) with an error of only 5.3%, which is an indication that of the possible sources of error discussed above, none proved significant enough to be a serious detriment to the experiment.

## 7 Conclusions and Recommendations

The purpose of this lab was to design, construct, and calibrate a full bridge strain gage transducer suitable for measuring levels of force, pressure, displacement, temperature, vibration, velocity, acceleration, etc, and to become familiarized with the use of transducers and strain gages. In the experiment, this was achieved by designing a tensiometer that would output a strain as a result of an input tension. The tensiometer, equipped with four strain gauges and connected to a P3 strain indicator, was put under load and values for strain were taken from the P3 indicator at even intervals of tension (see section 2a for detailed explanation of how the tensiometer was built and how it works).

Theoretical values for microstrain within the tensiometer were calculated by analyzing geometry and force equations. Algebraic manipulation was used to come up with one expression for microstrain as a function of only known variables, for increments of tension. This linear function was compared against the experimental results. Figure (14) shows the graphs of theoretical and measured results on the same set of axes, and it shows that the results from this experiment were very accurate to what was expected based on the theory. The equations of the lines for the P3 measured data and theoretical data are  $y = 0.622x - 2.16$  and  $y = 0.601x - 2.7$  respectively. Although not the exact same, these equations are very similar as seen by the values of their slopes and y-intercepts. In addition to this, looking at the finite analysis of the tensiometer, it shows a theoretical value for microstrain of  $6.347 \mu\epsilon$  at the centroid of the strain gauges. Compared to the calculated value of  $6.01 \mu\epsilon$  at the corresponding location, this shows that the theory is once again supported.

These discrepancies could be based on a number of things, including inaccuracies with the instron (relative zeroing, ambient noise in the room) due to how sensitive the device can be, or other sources such as material property estimates and simplifications with modeling. In conclusion, even with these multiple possible sources of error, the results from the experiment were accurately predicted by the theory presented. Although a successful experiment, there are some aspects of the tensiometer that could be improved upon. One prevalent source of error was not being able to secure the device to the Instron machine in a truly legitimate fashion. In the experiment, the ends of the cable were coiled and placed between clamps, and it was difficult to adjust to find the zero point of the Instron. Keeping the tensiometer on the correct plane without swaying was also difficult to do with consistency. Figuring out a proper way to secure the cable at each end would ensure greater accuracy and uniformity of measurements for multiple trials, and overall make the system more solid as a whole.

## 8 Acknowledgements

The authors would like to thank the University of Rhode Island Mechanical Engineering Department for providing us with the equipment and materials necessary to conduct this experiment.

## **Bibliography**

[1] A. Shukla, J.W. Dally. Instrumentation and Sensors For Engineering Measurements and Process Control. College Houses Enterprises LLC. 2013.

[2] Model P3 Strain Indicator and Recorder Instruction Manual. Vishay Micro-Measurements. March 2005.

[3] Hoffmann, Karl. Applying the Wheatstone Bridge Circuit. Hottinger Baldwin Messtechnik GmbH.

[4] Instron Series 5500 Load Frames Including Series 5540, 5560, 5580. Instron Corporation, 2005.

## **9 Appendices**

Designation	Description	Dimension mm (inch)
E	Crosshead thickness 5581/5582 5584/5585H	150 (6.0) 200 (8.0)
F	Controller height	120 (4.7)
G	Base beam height from floor With base extension 2910-061	480 (18.9) 780 (30.7)
H	Gap for feet - nominal setting	45 (1.8)
J1	Crosshead position 5581/5582 Minimum Maximum 5584/5585H Minimum Maximum	225 (8.9) 1460 (57.5)  278 (11.0) 1460 (57.5)
J2	Not applicable	
K	Overall depth	757 (29.8)
L	Front of base to test center	369 (14.5)
M	Motor cover height	362 (14.3)
N	Overall height With base extension 2910-061	2092 (82.4) 2392 (94.2)
P	Overall width	1307 (51.5)
Q	Coupling pin to base	59 (2.3)
R	Load cell pin or thread face to underside of crosshead 5581/5582 - with 2525-800 load cells (50/100kN)  5584/5585H - with Low Profile 2525-171/174 load cells	16 (0.7)  111 (4.4)
S	Width of controller	183 (7.2)
T	Clearance under base	112 (4.4)
U	Column depth	200 (7.8)

Figure (13) Addendum: Instron Model 5582 Dimensions [4]